THE JOURNAL OF PHYSICAL CHEMISTRY C

Article

pubs.acs.org/JPCC

Accurate Adsorption Thermodynamics of Small Alkanes in Zeolites. Ab initio Theory and Experiment for H-Chabazite

GiovanniMaria Piccini,[†] Maristella Alessio,[†] Joachim Sauer,*[,†] Yuchun Zhi,[§] Yuanshuai Liu,[§] Robin Kolvenbach,[§] Andreas Jentys,[§] and Johannes A. Lercher*[,§]

[†]Institut für Chemie, Humboldt-Universität zu Berlin, Unter den Linden 6, Berlin, Germany

[§]Department Chemie and Catalysis Research Center, Technische Universität München, Lichtenbergstrasse 4, 85748 Garching, Germany

Supporting Information

ABSTRACT: Heats of adsorption of methane, ethane, and propane in H-chabazite (Si/Al = 14.4) have been measured and entropies have been derived from adsorption isotherms. For these systems quantum chemical ab initio calculations of Gibbs free energies have been performed. The deviations from the experimental values for methane, ethane, and propane are below 3 kJ/mol for the enthalpy, and the Gibbs free energy. A hybrid high-level (MP2/CBS): low-level (DFT+dispersion) method is used to determine adsorption structures and energies. Vibrational entropies and thermal enthalpy contributions are obtained from vibrational partition functions for the DFT+dispersion potential energy surface. Anharmonic corrections have been evaluated for each normal mode separately. One-dimensional Schrödinger equations are solved for potentials obtained by (curvilinear) distortions of the normal modes using a representation in internal coordinates.

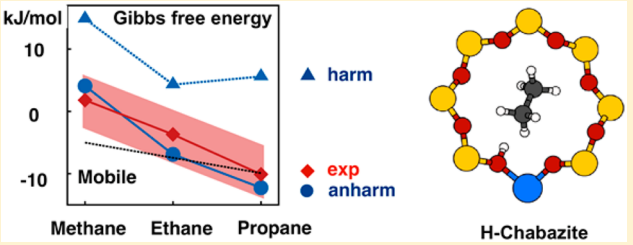

1. INTRODUCTION

A quantitative theory of heterogeneous catalysis requires accurate knowledge of thermodynamic functions for all elementary steps such as adsorption, chemical transformations, and desorption. For example, the compensation between increasing alkane adsorption energies in zeolites and increasing entropy loss[1] has been invoked to explain the variation of cracking rates with chain size.[2] Reliable methods for their calculations being missing, the role of entropy and enthalpy in stabilizing transition states in zeolite catalysis remained controversial.[3] Most often, adsorption entropies and desorption pre-exponential factors are estimated using simple models,[4] whereas experimental values for molecule−surface interactions are scarce.[1,5]

Statistical thermodynamics relates rate and equilibrium constants to free-energy changes for the formation of activated complexes (transition state theory) and products, respectively.[6] While it has been demonstrated that energy barriers and reaction energies for large chemical systems such as enzymes,[7] zeolites,[8−10] metal−organic frameworks,[11,12] and oxide surfaces[13−16] can be predicted with chemical accuracy, the ab initio prediction of free energy changes is more challenging. Sampling the potential energy surface by molecular dynamics[17,18] (e.g., umbrella sampling and thermodynamic integration, or (configurational-bias), Monte Carlo[19] requires millions of energy calculations to reach convergence. This limits these methods to systems for which good force fields are available, which is often the case in molecular biology.[17,18] For molecule−surface interactions force fields that describe both adsorption and reaction steps with sufficient accuracy for free-energy simulations are not available. Free energy simulations (e.g., alkane-zeolite systems) are limited to all-silica forms without catalytically active sites and assume rigid zeolite frameworks.[19,20]

The alternative approach, calculating free energies from vibrational partition functions, is standard for molecular systems.[6] It relies on the Taylor expansion of the high-dimensional potential energy surface around the equilibrium structure (minimum or transition structure). If the harmonic approximation is made, it becomes tractable even for systems with hundreds of atoms in the unit cell and has been applied to adsorption[12,21−26] and surface reactions.[9,27] While the force constants can be calculated directly from the ab initio potential energies without fitting, the main limitation of the harmonic oscillator model is that low vibrational frequencies make the largest contribution to the entropies (see ref 6, section 10.5.2) and that relatively small errors on these frequencies lead to large errors in the entropy term. This is particularly true for the low-frequency modes arising from the conversion of the three translational and three rotational degrees of freedom into six molecule-surface vibrations (i.e., in more or less hindered translations and rotations) and soft vibrational modes of the solid material (e.g., in zeolite frameworks).[28,29] Sometimes it is then a better approximation to assume that the molecules are freely rotating on the surface (H_2 and CH_4 in metal−organic

Received: February 20, 2015
Published: March 10, 2015

DOI: 10.1021/acs.jpcc.5b01739
J. Phys. Chem. C 2015, 119, 6128−6137

frameworks)[11,12] or that free rotation and translation is preserved for some degrees of freedom, depending on the nature of the molecules [alkanes on MgO(001)[15] and "mobile" adsorption of alkanes in zeolites[22]].

In the area of adsorption and catalysis, development and validation of new computational protocols is hampered by the scarcity of reliable experimental data needed for the assessment of the results. Therefore, we provide experimental benchmark data (enthalpies, entropies, and free energies) for the adsorption of methane, ethane, and propane in the acidic zeolite chabazite, H-SSZ-13. Due to its limited unit cell size, the chabazite framework is well-suited for computational studies,[10,28−32] and in its aluminum phosphate form, it is industrially used as a catalyst in methanol to olefin processes.[33] The important role of a preceding adsorption step for the catalytic conversion of molecules at surfaces has been convincingly demonstrated by Haag for alkane cracking on the acidic zeolite H-ZSM-5.[34]

In the present contribution, the measured heats and equilibrium constants as well as entropies and free energies of adsorption determined from the former are reproduced by our calculations within chemical accuracy limits (±1 kcal/mol ≈ 4.2 kJ/mol). This could only be achieved (i) by combining second-order Møller−Plesset perturbation theory (MP2) for cluster models with density functional theory (DFT) for the periodic system when calculating energies[35,36] and (ii) by calculating vibrational partition functions from anharmonic vibrational frequencies,[28,29,37] with curvilinear sampling of one-dimensional potentials for each degree of freedom,[29] as suggested by Gordon and co-workers for molecules.[38−40]

The present results differ substantially from the previous study of Piccini and Sauer[28] in two respects: (i) MP2 corrections which lower the DFT(+dispersion) energies by about 10 kJ/mol have not been made in the previous study. (ii) Previously, anharmonic potentials were calculated along rectilinear distortions, which yielded anharmonicity corrections to entropies that had the opposite sign. This had been noted,[28] but in the absence of experimental results for the same systems, a definitive conclusion was not reached. Now, having the missing measurements performed, we are able to show that chemical accuracy has been reached in ab initio calculations of both enthalpies and the entropy contribution to free energies.

The computational protocol presented here has the potential to become a standard tool in ab initio studies of molecule−surface interactions. It will make simple entropy models for molecule−surface interactions like the ones mentioned above[11,12,15,22] obsolete. It is feasible for all systems that are accessible for the harmonic approach, as only force calculations for additional points of the potential are needed. Applications to adsorption of gases and gas mixtures in nanoporous materials (MOFs, zeolites) and to hydrocarbon reactions in zeolites are in progress.

2. SAMPLES AND EXPERIMENTS

2.1. Samples. A chabazite sample with a Si/Al ratio of 14.4 (determined by atom absorption spectroscopy) was obtained from Chevron Energy Technology Co. in the Na^+ form and transferred into the proton form by ion exchange with NH_4NO_3 and subsequent calcination at 450 °C for 2 h. The concentration of acid sites determined by temperature-programmed desorption of NH_3 was 1.0 mmol/g, which is in prefect agreement with the value expected from the Si/Al ratio (1.0 mmol/g). For further details, see the Supporting Information.

2.2. Gravimetric/Calorimetric Sorption Experiments. The sorption isotherms of methane, ethane, and propane were measured on a Setaram TG-DSC 111 instrument. The zeolite was activated with a heating rate of 10 K min^{-1} in vacuum ($p < 10^{-7}$ mbar) to 723 K, maintaining the final temperature for 30 min. The weight increase and the thermal flux were measured during equilibration with the sorbate at 313, 333, 343, and 363 K up to a partial pressure of 1 bar for ethane and propane. Because of its weak binding leading to a very low coverage above room temperature, the adsorption was carried out at 303 K for methane. The heat of adsorption was determined by integration of the heat signal observed during the stepwise increase of the pressure of the adsorbing gas. The uptake was determined after equilibration for 40 min. Figure 1 shows the isotherms for ethane and propane at 313 K and Figure 2 the heats of adsorption for methane, ethane, and propane.

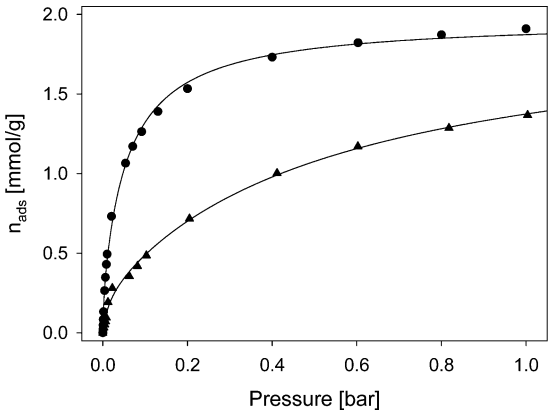

Figure 1. Sorption isotherms of ethane (▲) and propane (●) on chabazite at 313 K together with the fits using the dual site Langmuir model.

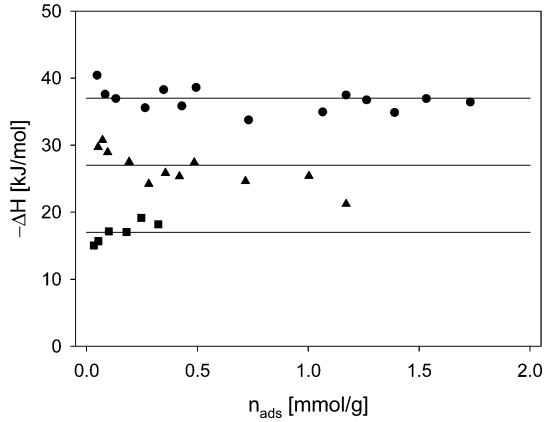

Figure 2. Adsorption enthalpy of methane (■), ethane (▲), and propane (●) on H-chabazite.

Two Langmuir isotherms were required to describe the sorption of the alkanes on chabazite (see Supporting Information). The contribution at low loadings (n_{ads} < 0.25 mmol/g) is assigned to the sorption at defect (Lewis acid) sites. It is associated with the higher heat of adsorption observed at very low coverages, presumably at Lewis acid sites (see Figure 2). The second isotherm (main contribution) is attributed to

DOI: 10.1021/acs.jpcc.5b01739
J. Phys. Chem. C 2015, 119, 6128−6137

localized adsorption on Brønsted acid sites in the chabazite pores.

The mode of interaction has been quantitatively assessed using IR spectroscopy. The IR spectrum of the activated zeolite showed two groups of bands. The first consists of a relatively broad band at 3734 cm^{-1}, and a nonresolved band of low intensity at 3745 cm^{-1}. The latter band is attributed to SiOH groups terminating the zeolite crystal, while the band at 3734 is attributed to SiOH groups terminating defects in the inner of the zeolite pores. The other group consisting of OH stretching bands at 3612, 3597, and 3586 cm^{-1} is attributed to SiOHAl Brønsted acid hydroxyl groups in CHA. Following Bordiga et al.,[41] the SiOHAl bands at 3612 and 3586 cm^{-1} are attributed to the OH groups at the O(1) and/or O(2) positions in the 8-membered ring and OH groups at the O(3) position, facing a 6-ring window. The well-developed shoulder at 3597 cm^{-1} is tentatively attributed to the O(2) or the O(4) position of CHA.

The adsorption of the alkanes led to a simultaneous decrease of the intensity of the bands at 3612 and 3597 cm^{-1}, showing that both are accessible and interact with alkanes. The band at 3586 cm^{-1}, attributed to the OH group at the O(3) position did not markedly change in intensity, indicating a significantly weaker interaction than with the other OH groups. It is worth mentioning that the inability of OH groups pointing into six-membered rings to interact with alkanes has also been observed for zeolite Y,[42] confirming the attribution of the band at 3586 cm^{-1} to the O(3) position. Upon interaction with the alkanes, a broad band with a maximum at 3537 cm^{-1} appeared, attributed to hydrogen bonding of the alkane via SiOHAl polarized C−H groups. The parallel decrease of the bands of the free OH groups and the parallel increase of the complex broad band of the perturbed OH vibrations suggests an equal strength of both OH groups.[43] The pressure independent position of the perturbed OH vibration indicates that a relatively localized interaction between the hydrocarbons and the Brønsted acid sites was formed and that the local orientation of the molecules was not affected by the partial pressure until a high coverage of these sites was reached.

The modest decrease of the intensity of the SiOH at 3735 cm^{-1} and appearance of the associated perturbed OH vibrations at 3720 cm^{-1}, paralleling the adsorption on Brønsted acid sites indicates that these SiOH groups are predominately located at defects inside the pores and laterally interact with hydrocarbon molecules adsorbed at Brønsted acid sites.

The linear correlation between the concentration of adsorbed species and the integral intensities of the CH stretching bands (Supporting Information, Figure S5) as well as the integral intensity of the OH stretching vibrations associated with the bridging OH groups (Figure S6) point to a ratio of one adsorbed molecule per strongly Brønsted acidic bridging OH group for the range of coverages explored by DFT.

Using the heat of adsorption (Figure 2) and adsorption equilibrium constant of the Langmuir isotherm corresponding to molecules that do not interact with the Lewis acid sites, the Gibbs−Helmholtz equation yields the standard adsorption entropy.

$$TS_T^0 = RT \ln K_T + H_T^0 \quad (1)$$

Table 1 shows these enthalpies and entropies of adsorption together with the data of Barrer and Davies[44] for enthalpies and entropies of adsorption derived via the isotherms measured at varying temperatures.

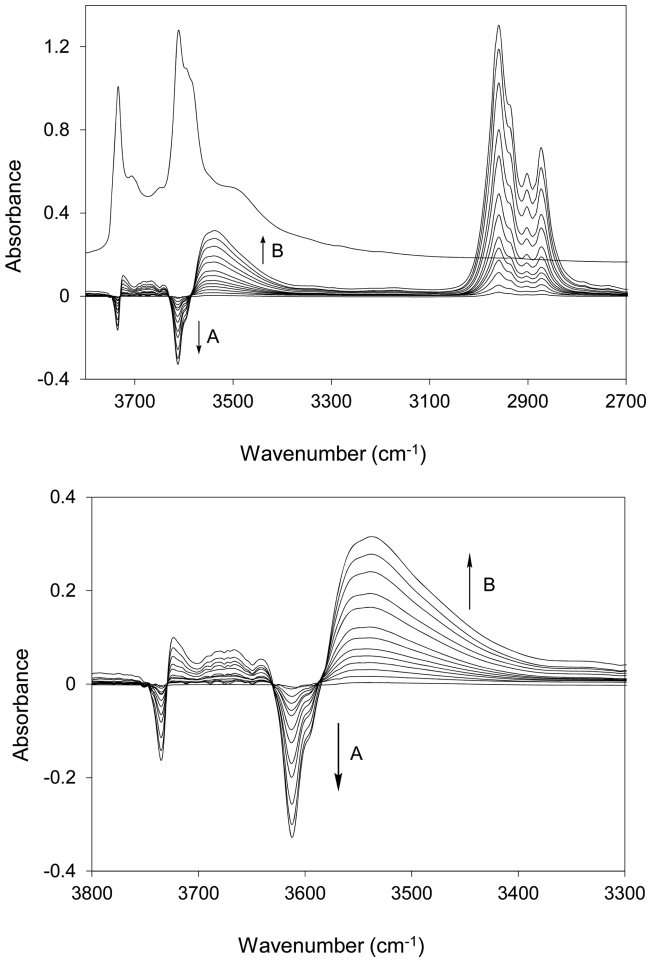

Figure 3. Difference in the IR spectra after adsorption of propane at partial pressures between 10^{-4} and 10^{-2} bar at 313 K. The bottom figure is an enlarged version of the variation in the IR spectra of the OH stretching region. The arrows indicate the changes with increasing pressure. (A) Decreasing intensity because of interactions with SiOH (3734 cm^{-1}) and SiOHAl (3612, 3597 cm^{-1}) groups. (B) Increasing intensity because of stretching vibrations of hydrogen-bonded SiOH groups at 3720 and 3663 cm^{-1}; the latter being attributed to hydrogen-bonded SiOH at defect sites as well as to hydrogen-bonded SiOHAl groups at 3537 cm^{-1} with a shoulder at 3555 cm^{-1} (above 10 mbar propane equilibrium pressure, an additional band at 3712 cm^{-1} appeared, indicating a somewhat stronger interaction with SiOH groups).

3. METHODS AND MODELS

3.1. Energy Calculations and Structure Optimization.

We use a hybrid high-level quantum mechanics: low-level quantum mechanics mechanical embedding approach[35,36] that combines second-order Møller−Plesset perturbation theory (MP2) for a cluster model of the adsorption complex as high-level method with density functional theory (DFT) for the full periodic structure of the adsorbed molecule−surface system.

The hybrid QM:QM energy is defined by a subtractive scheme:

$$\begin{aligned} E_{\mathrm{HL:LL}}(\mathrm{pbc}) &= E_{\mathrm{LL}}(\mathrm{pbc}) - E_{\mathrm{LL}}(C) + E_{\mathrm{HL}}(C) \\ &= E_{\mathrm{HL}}(C) + \Delta_{\mathrm{LR}}(\mathrm{pbc}, C) = E_{\mathrm{LL}}(\mathrm{pbc}) + \Delta_{\mathrm{HL}}(C) \end{aligned} \quad (2)$$

where $E_{\mathrm{LL}}(\mathrm{pbc})$ is the low-level energy of the adsorbed molecule−surface system, including periodic boundary con-

DOI: 10.1021/acs.jpcc.5b01739
J. Phys. Chem. C 2015, 119, 6128−6137

Table 1. Standard Enthalpy, $\Delta H°$ (kJ/mol), and Entropy, $\Delta S°$(J/mol K) for the Adsorption of Alkanes in Two H-Chabazites with Different Si/Al Ratio at Temperature T

	H-SSZ-13 (Si/Al = 14.4), this work				H-chabazite (Si/Al = 2.6)[a]		
	Θ_s[b]	T	$\Delta H°$	$\Delta S°$	T	$\Delta H°$	$\Delta S°$
methane	1.30	303	−17.0	−63.5	273.2	−20.4	−64.9
ethane	1.99	313	−27.5	−76.1	313.2	−30.8	−70.7
propane	1.97	313	−37.6	−87.7	323.2	−37.3	−67.4

[a]Barrer and Davies, ref 44. [b]Saturation coverage [mmol/g].

ditions, $E_{LL}(C)$ is the low-level energy for the cluster model of the adsorbed molecule on the surface, and $E_{HL}(C)$ is the high-level energy for the same finite size cluster models. The result can be viewed at as a high-level calculation for the cluster model, $E_{HL}(C)$, to which a long-range correction,

$$\Delta_{LR}(\text{pbc}, C) = E_{LL}(\text{pbc}) - E_{LL}(C) \tag{3}$$

evaluated at the low-level, has been added, or a low-level calculation with periodic boundary conditions for the full structure, to which a high-level correction,

$$\Delta_{HL}(C) = E_{HL}(C) - E_{LL}(C) \tag{4}$$

evaluated for the cluster model, has been added. The dangling bonds of the cut-out defining the high-level cluster are terminated with hydrogen "link" atoms.[45] Structure optimizations are performed on the combined potential energy surface defined by eq 1 with forces calculated by the same subtraction scheme,[45,46]

$$f_{i,\text{HL:LL}}(\text{pbc}) = f_{i,\text{LL}}(\text{pbc}) - f_{i,\text{LL}}(C) + f_{i,\text{HL}}(C) \tag{5}$$

The (high-level) QM [e.g., MP2 binding energies are counterpoise corrected (CPC) for the basis set superposition error (BSSE) of the atom-centered basis sets used].[47] On the BSSE-free potential energy surface, an extrapolation to the complete basis set (CBS) limit is performed,[48] which uses Dunning's correlation consistent basis sets with two consecutive cardinal numbers $X = 2$ (double-ζ, D) and $X = 3$ (triple-ζ, T in the present case). For the Hartree−Fock (HF) part, an exponential extrapolation scheme is applied[48,49]

$$E_{\text{HF},X} = E_{\text{HF},\infty} + A \exp(-1.5X) \tag{6}$$

while an inverse power law is used for the correlation energy[50]

$$E_{\text{corr},X} = E_{\text{corr},\infty} + AX^{-3} \tag{7}$$

When used to calculate forces, this CPC−CBS scheme allows structure optimizations on the BSSE free basis set extrapolated potential energy surface. Its use as a high-level method in the subtraction scheme for embedded cluster calculations defines a multilevel method that avoids artifacts in the equilibrium structure prediction as for example a typically too short distance between the adsorbed molecule and the surface.

Hybrid QM:QM calculations have been performed using the development MonaLisa program written in C++ programming language.[51] MonaLisa incorporates the main features of QMPOT software[46] previously used and benefits from the flexibility and modularity of the object-oriented coding. The general purpose of MonaLisa is locating minima and transition structures on multilevel PES. It includes a variety of independent interfaces to allow the communication between the internal optimizer and the external computational chemistry programs that provide energies and gradients. For this present MP2/CPC−CBS:DFT+D coupling MonaLisa provides interfaces to TURBOMOLE and VASP programs.

Plane wave DFT calculation have been performed using the VASP program[52] (5.2.12 version) with a 600 eV energy cutoff requiring an energy difference between two consecutive SCF cycles of 10^{-8} eV/cell. The PBE[53] functional has been employed, and dispersion contributions are described by a damped $1/r^6$-term using Grimme's "D2" parameters.[54] We will refer to this method as PBE+D.

MP2 calculations have been carried out using the resolution of identity (RI)-CC2 module[55] available in version 6.5 of the TURBOMOLE program.[56] For all atoms in the system, Dunning's correlation-consistent polarized valence basis sets (cc-pVXZ) of systematic increasing quality from X = D to X = T[57,58] have been used and the 1s frozen-core approximation has been applied.

3.2. Vibrational Partition Functions and Frequency Calculation. Entropies and thermal enthalpy contributions are evaluated for the low-level (PBE+D) potential energy surface from vibrational partition functions, q_a, approximated as finite sums over vibrational states i (k_B is the Boltzmann constant and T the temperature)

$$q_a \approx \sum_{i=0}^{m} e^{-e_i/k_B T} \tag{8}$$

The quantum diagonal anharmonic energy levels obtained are used to evaluate anharmonic contributions to vibrational partition functions. We follow the procedure described before.[28,29] If analytical second derivatives are not available as it is the case for plane wave codes used in this study, harmonic force constants are calculated as numerical derivatives of Cartesian forces. From the latter, a set of normal modes {Q} is derived that relates to the Cartesian displacement coordinates through

$$\Delta x = SQ \tag{9}$$

Having the normal modes, a new set of harmonic frequencies is calculated, also using finite differences of forces but displacing the atoms along the normal modes of vibration. This yields improved harmonic frequencies, and if enough points along each normal mode are used to calculate the forces, an anharmonic one-dimensional model potential is derived for each normal mode by fitting the points on the PES. To minimize anharmonic couplings between the one-dimensional oscillators, expressing the normal modes in curvilinear coordinates (such as internals) is mandatory when making finite distortions.[38−40,59]

Harmonic and anharmonic frequencies in normal mode coordinates have been calculated using the program EIGEN_HESS_ANHARM_INT.[28] The program written in F90 interfaces with VASP[60] to get total energies and gradients from single-point calculations and the Hessian matrix to get

DOI: 10.1021/acs.jpcc.5b01739
J. Phys. Chem. C 2015, 119, 6128−6137

frequencies from Cartesian finite differences and the corresponding eigenvectors. Thermodynamic properties such as translational, rotational, harmonic, and anharmonic energy and entropy contributions were obtained using the local F90 program THERMO.

3.3. Models. The acidic chabazite zeolite has been modeled by a supercell of dimensions a = 18.90 Å, b = 9.44 Å, c = 9.29 Å, α = 94.0051, β = 94.8903, and γ = 95.3793 degree, which is obtained by doubling the triclinic unit cell along the lattice vector a and which contains two acidic Brønsted sites (Si/Al ratio 11/1), see Figure 4. This ensures that lateral interactions

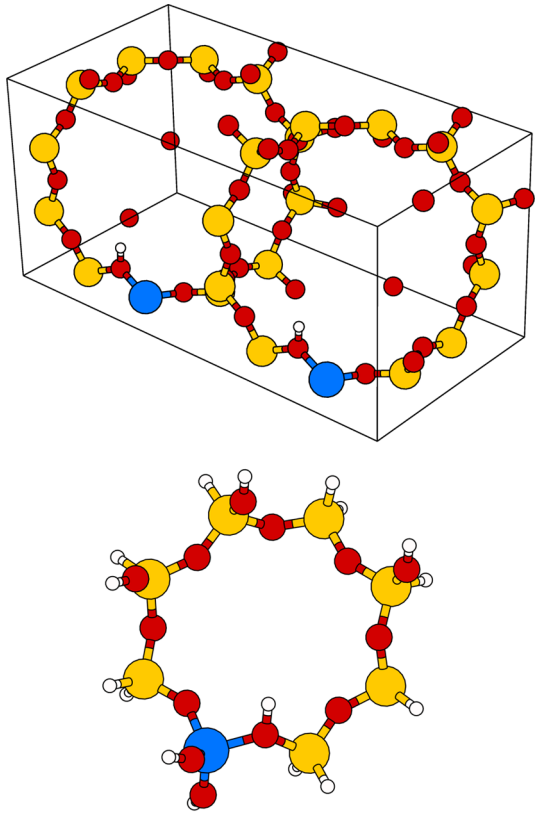

Figure 4. (Top) H−CHA 2a supercell showing the acidic hydrogen in position O2, an oxygen atom that is shared by two 8-membered rings and one 4-membered ring. (Bottom) $8T_{11H}$ cluster model employed in the hybrid MP2:DFT+D calculations. Color key: yellow, silicon; red, oxygen; blue, aluminum; and white, hydrogen.

between adsorbed molecules are negligible at half coverage (θ = 0.5) and that converged electronic structures are obtained for Γ-point-only calculations. This is the structural model adopted for the PBE+D calculations (normal-mode optimizations and frequency calculations).

For the hybrid QM:QM optimization, the low-level (PBE+D) calculations have been performed on a larger supercell to avoid contact between the link atoms of clusters in neighboring cells. The new supercell obtained by duplicating the cell of Figure 4 along the c direction has the following crystallographic parameters: a = 18.90 Å, b = 9.44 Å, c = 18.45 Å, α = 94.0051, β = 94.8903, and γ = 95.3793 degrees.

The bottom part of Figure 4 shows the $8T_{11H}$ cluster employed in the low- and high-level calculations. Following the previously introduced nomenclature,[9,35,36] it consists of eight tetrahedra with 11 Si−H terminating groups, while all other link atoms saturate oxygen atoms and thus form terminating OH groups, 2 at the Al and 3 at the Si atoms.

For plane wave DFT calculations on methane, ethane, and propane molecules in the gas phase as well as on cluster models employed in the low-level (DFT+D) part of the QM:QM scheme, the systems have been put in the center of a cubic box of 20 Å to prevent Coulomb interactions with their periodic images. This allows also Γ-point only sampling of the Brillouin zone.

4. COMPUTATIONAL RESULTS

4.1. Ab Initio Energy Calculations. The adsorption complexes of methane, ethane, and propane with the acidic active site of H−CHA have been preoptimized on the PBE+D potential energy surface using normal-mode coordinates instead of Cartesians.[28] Subsequently, these structures reported in ref 28 have been refined using a hybrid approach that combines high-level MP2/CPC−CBS(D,T) energies with low-level PBE+D/plane wave energies for the periodic systems within a subtractive QM:QM scheme,[35,36,61] as described in Energy Calculations and Structure Optimization.

Figure 5 shows the results as a cut-out of the periodic structure. As a common structural motif, the acidic hydrogen in

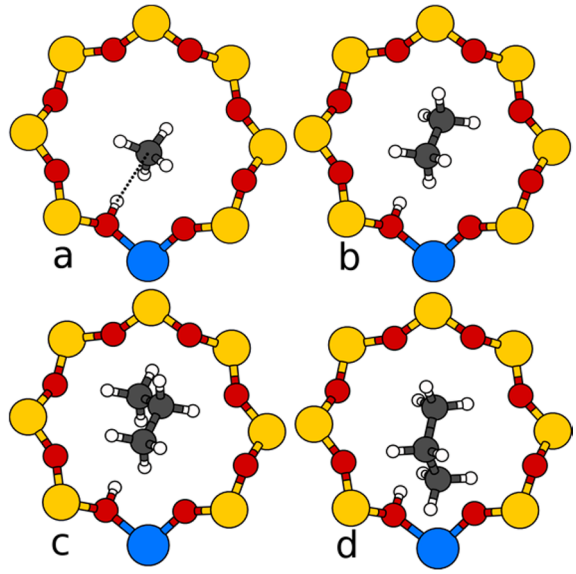

Figure 5. Adsorption complexes of (a) methane, (b) ethane, (c) propane via primary carbon, and (d) propane via secondary carbon with the acidic group at HO(2) in an 8-membered ring of H−CHA.

the O(2) position points toward the carbon atom. Table 2 reports the OH···C distances between the acidic surface OH group and the closest C atom of the alkane molecule. Compared to the hybrid MP2:PBE+D results, PBE+D yields significantly shorter molecule−surface distances in accord with

Table 2. OH···C Bond Distances (pm) of the Adsorption Complexes

method	methane	ethane	propane	
			C(1°)[a]	C(2°)[a]
PBE+D[b]	215	214	213	218
MP2/CPC−CBS(D,T):PBE+D	228	221	219	219

[a]Adsorption via primary and secondary carbon, respectively. [b]Ref 28.

DOI: 10.1021/acs.jpcc.5b01739
J. Phys. Chem. C 2015, 119, 6128−6137

substantial overbinding. The PBE+D adsorption energies in Table 3 are 9.4 to 14.2 kJ/mol more binding than the hybrid MP2:PBE+D results. The PBE+D results for the periodic model at the hybrid MP2:PBE+D structure hardly differ from the PBE+D energies for the structures optimized at this level.

The hybrid MP2:PBE+D results for methane, ethane, and propane (primary C attack) follow the relation (in kJ/mol)

$$\Delta E = 14.7 + 10.7N_C \quad (10)$$

In addition to the total energies, Table 3 shows also the individual contributions to the hybrid QM:QM model for the adsorption structures considered. The MP2 energies for the cluster models are all in between 21.2 and 22.3 kJ/mol, and all the chain length variation stems from the long-range correction, Δ_{LR}, evaluated at the PBE+D level.

Table 3. Electronic Adsorption Energies Obtained with the Hybrid MP2/CPC−CBS(D,T): PBE+D Method, And Energy Contributions for the Periodic Model, S, and the Cluster Model, C, Obtained with Different Methods for Alkane Adsorption in H−CHA (kJ/mol)[a]

		methane	ethane	propane	
				C(2°)[b]	C(1°)[b]
E(pbc)[c]	PBE+D[c]	−32.3	−43.4	−59.4	
E(pbc)[d]	PBE+D[d]	−34.72	−45.78	−57.32	−58.30
E_{LL}(pbc)	PBE+D//MP2:PBE+D[e]	−33.02	−44.15	−58.47	−56.89
	PBE	−8.08	−7.84	−7.84	−8.32
	D	−24.94	−36.31	−50.63	−48.57
Δ_{LR}	PBE	0.53	−4.61	−5.66	−4.10
	D	−4.51	−10.44	−19.12	−17.73
	PBE+D	−3.98	−15.05	−24.78	−21.83
E_{HL}(C)	MP2//MP2:PBE+D[e]	−21.36	−21.17	−21.87	−22.30
Δ_{HL}		7.68	7.93	11.82	12.76
$E_{HL:LL}$(pbc)[f]		−25.34	−36.21	−46.65	−44.13
E(pbc)[g]	MP2//PBE+D[g]	−22.4	−35.1	−48.4	

[a]Long-range and high-level corrections, Δ_{LR} and Δ_{HL}, respectively, are also given (see eqs 2−4 for definitions). [b]Adsorption via primary and secondary carbon atom, respectively. [c]PBE+D at the PBE+D optimized structure, ref 10. [d]PBE+D at the PBE+D optimized structure, ref 28. [e]At the hybrid MP2:PBE+D optimized structure. [f]Total hybrid MP2:PBE+D. [g]Single-point MP2 at the PBE+D optimized structure, ref 10.

4.2. Thermodynamic Functions. Table 4 shows the thermodynamic functions for the adsorption of the methane, ethane, and propane in H−CHA at experimental conditions (303 K for methane and 313 K for ethane and propane, 0.1 MPa) for half coverage (θ = 0.5). Comparison is made between the results obtained from harmonic frequencies (harm), and from anharmonic frequencies derived from curvilinear distortions (anharm). There are substantial differences compared to the corresponding results in Table 4 of ref 28, which are due to the use of rectilinear distortions in that study. To get consistent results, anharmonic corrections have been applied to the vibrations of the adsorption complex, the unloaded chabazite, and the alkane molecules. Since analytical second derivatives are not available, harmonic force constants are obtained by numerical differentiation of forces resulting from normal mode distortions along internal coordinates. Thermal contributions to the total energies are calculated from the translational, rotational, and vibrational (harmonic or anharmonic) partition functions. Whereas the electronic energies are the hybrid MP2/CPC−CBS(D,T):PBE+D results (see Table 3), the frequencies are obtained from the PBE+D potential energy surface.

The calculated thermodynamic functions are compared with measured values (Gravimetric/Calorimetric Sorption Experiments). Figures 6 and 7 show the experimental data points (red ◆) with bars that indicate the chemical accuracy range (i.e., the range of ±1 kcal ≈4.2 kJ/mol). The thermodynamic functions calculated using anharmonic frequencies with internal coordinate distortions are all within the chemical accuracy range of the experimental data. The deviations of the T DS term are all smaller than 1 kJ/mol, and for methane, ethane, and propane adsorbed with the primary carbon atom, the deviations between calculated and experimental data are 1.8, −2.7, and −2.9 kJ/mol, respectively, for the enthalpy, and 1.9, −3.2, and −2.1 kJ/mol, respectively, for the Gibbs free energy.

The results for propane adsorption via the secondary carbon atom have been excluded from Figures 6 and 7 because the entropy term and, hence, the Gibbs free energy deviate significantly from the experimental data. Due to the strong interaction of the propane methyl groups with the zeolite framework, highly entropic motions such as hindered translations and rotations are way stiffer then in the case of primary

Table 4. Zero-Point Vibrational Energies (ZPVE), Energies at Zero Kelvin (ΔE_0), Thermal Enthalpy Contributions ($\Delta H - \Delta E_0$), Enthalpy (ΔH), Entropy Term ($-T\Delta S$), and Gibbs Free Energy (ΔG) for the Adsorption of Methane, Ethane, and Propane in H−CHA at Experimental Conditions (303 K for Methane, 313 K for Ethane and Propane, 0.1 MPa, θ = 0.5) Calculated Using Harmonic Internal Normal Mode Distortions (Harm), Anharmonic Internal Coordinates Distortions (Anharm), and Experimental Data (Exp), All in kJ/mol

	methane			ethane			propane				
							C(1°)		C(2°)		
	harm	anharm	exp[a]	harm	anharm	exp[a]	harm	anharm	harm	anharm	exp[a]
ZPVE	5.72	5.49	–	2.43	2.80	–	4.09	1.59	1.51	1.93	–
ΔE_0	−19.62	−19.85	–	−33.78	−33.41	–	−42.56	−45.06	−42.62	−42.20	–
$\Delta H - \Delta E_0$	−0.06	4.68	–	0.68	3.23	–	−0.14	4.59	2.89	3.24	–
ΔH	−19.68	−15.17	−17.0	−33.10	−30.18	−27.5	−42.70	−40.47	−39.73	−38.96	−37.6
$-T\Delta S$	34.53	19.25	19.2	37.42	23.28	23.8	48.31	28.22	42.55	40.49	27.5
ΔG	14.86	4.09	2.2	4.31	−6.90	−3.7	5.61	−12.26	2.82	1.52	−10.2

[a]Cf. Table 1.

DOI: 10.1021/acs.jpcc.5b01739
J. Phys. Chem. C 2015, 119, 6128−6137

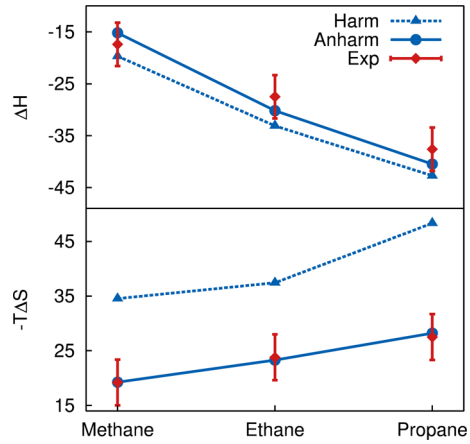

Figure 6. Enthalpy, ΔH, entropic term, $-T\Delta S$ and Gibbs free energy, ΔG, for the adsorption of methane, ethane and propane in H−CHA at experimental conditions (303 K for methane, 313 K for ethane and propane, 0.1 MPa, $\theta = 0.5$) calculated using harmonic internal normal mode distortions (Harm), anharmonic internal coordinates distortions (Anharm) and experimental data (Exp), all in kJ/mol.

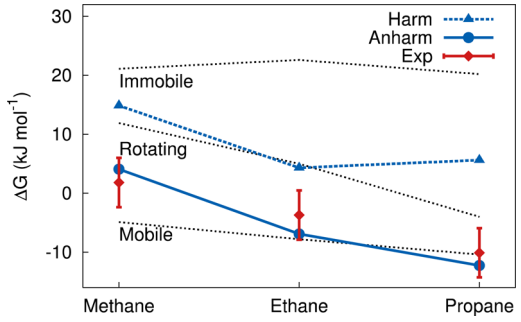

Figure 7. Gibbs free energy, ΔG (kJ/mol), for the adsorption of methane, ethane, and propane in H−CHA at experimental conditions (303 K for methane, 313 K for ethane and propane, 0.1 MPa, $\theta = 0.5$) calculated using harmonic internal normal mode distortions (Harm), anharmonic internal coordinates distortions (Anharm), experimental data, and simplified adsorption models (black dashed lines for immobile, rotating, and mobile models, respectively).

carbon adsorption, resulting in a much lower entropy of the adsorption complex. This disfavors adsorption via the secondary carbon compared to adsorption via the primary carbon atom. This feature has been observed also in molecular dynamics simulations. Bučko et al.[32] have shown that the probability of adsorbing a propane molecule in H−CHA via a primary carbon atom is about seven times higher than adsorbing it via a secondary one. The present results show that the origin of this unfavorable adsorption configuration is entropic as the enthalpy does differ strongly between the two adsorption structures. For the proper description of this effect, anharmonic contributions are essential. Within the harmonic approximation, the opposite conclusion is reached. Adsorption via the secondary carbon is favored over adsorption of the primary one.

5. DISCUSSION

The effect of anharmonicity on the entropy term is enormous, of the order of 15 to 20 kJ/mol. A very large effect is also seen for the thermal enthalpy contributions, which increase by 4.7 (methane), 2.6 (ethane), and 4.7 (propane) kJ/mol. The low frequency/large amplitude modes associated with the hindered translations and rotations of the adsorbed molecule, the floppy vibrations of the zeolites framework[62−65] and also the possible internal rotations of methyl groups in ethane and propane are far from being properly described by a parabolic model potential. The accurate estimation of the adsorbed state entropy given by treating all the vibrations as anharmonic is key to understanding why zeolites are such excellent adsorbent materials. The floppy vibrational structure of zeolites also favors the diffusion of molecules into the pores.[19,66] Since soft vibrations can couple with the surface modes, the vibrational structure of the whole crystal framework changes consistently with the presence of the adsorbate. This means that the crystal adapts its structure to accommodate the molecule weakening the strength of some bonded interactions (mainly collective angle bending and torsions), which give rise to a highly entropic adsorbed state. We note that the computational expense of the anharmonicity calculation is just a multiple (factor of 10 at most) of the calculation of harmonic frequencies. That means whenever a harmonic calculation is feasible, the anharmonic calculation will also be feasible. The bottleneck is rather finding the appropriate internal coordinates for the curvilinear representation of the normal modes, which is not always easy.

Figure 7 shows the results for the Gibbs free energies and compares them with results which use simple models proposed by Tait et al.[15] for estimating adsorption entropies. For the desorption of linear alkanes from the MgO(100) surface, the adsorption entropies have been calculated (i) for an immobile adsorbate model, where no translations or rotations are allowed in the adsorbed state, (ii) for a rotating adsorbate, where only rotations along the adsorbate principal axis of inertia are allowed (3 for a nonlinear molecule), and (iii) for a mobile adsorbate, where 2D translations and a specific number of rotations are allowed, depending on the nature of the molecule.[15] In our case, this number is 3 for methane, 2 for ethane, and 1 for propane. The "mobile adsorption model" is in better agreement with the experimental result and also a better approximation to our anharmonic calculated result than our calculated result using the harmonic approximation.

In the past, we have shown that chemical accuracy can be reached for adsorption energies of the CO/MgO(001)[13,14] and CH_4/MgO(001) systems.[15,16] The present paper aims at extending the list of thermodynamic reference systems by providing experimental and computational thermodynamic benchmark data.

In contrast to quantum chemical calculations, experiments do not yield energies of adsorption defined as differences between the bottom of the respective potential wells. However, the difference between the experimental enthalpy (Table 1) and the sum of our calculated thermal enthalpy contributions and zero-point vibrational energies,

$$\Delta E(\text{ref}) = \Delta H_T(\text{exp}) - [[\Delta H_T - \Delta E_0(\text{PBE} + \text{D})] - \text{ZPVE}(\text{PBE} + \text{D}) \quad (11)$$

yields a reference value for the (electronic) energies of adsorption, ΔE (ref). Table 5 shows that the difference between ΔH_T (exp) and ΔE (ref) is as large as 10.2, 6.0, and 6.2 kJ/mol for methane, ethane, and propane, which should not be ignored when testing different quantum chemical methods for calculating molecule−surface interactions. Thermal contributions are as important as zero-point vibrational energies. The harmonic approximation recovers only part of this

DOI: 10.1021/acs.jpcc.5b01739
J. Phys. Chem. C 2015, 119, 6128−6137

Table 5. Energies of Adsorption, ΔE (exp), Derived from Experimental Heats of Adsorption, ΔH_T (exp), and Calculated (PBE+D) Thermal Corrections, $\Delta H_T - \Delta E_0$, and Zero-Point Vibrational Energies, ZPVE, All in kJ/mol

H−CHA	methane	ethane	propane
ΔH_T (Exp)	−17.0	−27.5	−37.6
$\Delta H_T - \Delta E_0$ (PBE+D)	4.7 (−0.1)[a]	3.2 (0.7)[a]	4.6 (−0.1)[a]
ZPVE (PBE+D)	5.5 (5.7)[a]	2.8 (2.4)[a]	1.6 (4.1)[a]
ΔE (ref)	−27.2 (−23.6)[a]	−33.5 (−30.6)[a]	−43.8 (−41.6)[a]

[a]In parentheses: harmonic approximation.

difference, 5.6, 3.1, and 4.0 kJ/mol, respectively, and in particular fails to describe thermal contributions properly.

For our best hybrid MP2:PBE+D adsorption energies (Table 3, last row), the deviations from the reference values (Table 5, last row) are 1.8, −2.7, and −2.9 kJ/mol for methane, ethane, and propane, respectively, all well within the chemical accuracy range of ±4.2 kJ/mol. The remaining deviation is not due to higher-order correlation effects as test calculations for the CH_4/H−CHA system have shown. The difference between CCSD(T) and MP2 is −0.4 kJ/mol only.

The single-point MP2/pane wave//PBE+D results of Göltl et al.[10] show slightly larger deviations from the reference values, 4.8, −1.6, and −4.8 kJ/mol for methane, ethane, and propane, respectively, but are still close to chemical accuracy limits. The availability of experimental values and reliably calculated nuclear motion and thermal corrections provides additional support for the conclusion of Göltl et al.[10] regarding the performance of different methods. Using our reference energies, the random phase approximation (RPA) based on DFT underestimates the binding by 10 to 17 kJ/mol, and only the combination of the exchange energy from self-consistent Hartree−Fock calculations with the RPA correlation energy calculated with PBE orbitals ("hybrid RPA-HF" method) yield very accurate results with deviations of 0.4, 1.1, and 0.0 kJ/mol for methane, ethane, and propane. Since structures optimized with PBE+D have been used, these small deviations may involve some error cancellation. The van der Waals functionals applied by Göltl et al.[10] overestimate the binding quite strongly with increasing deviations of about −10 kJ/mol for methane, −24 kJ/mol for ethane, and −31 kJ/mol for propane. The PBE+D calculations (D2 parametrization) overestimate binding with deviations of −7.5, −12.3, and −13.5 kJ/mol for methane, ethane, and propane, respectively. While an alternative parametrization of the atom−atom C_6/R^6 term (Tkatchenko-Scheffler) shows a similar performance for methane (−7.4 kJ/mol deviation), the overbinding increases when passing to ethane and propane with deviations of −18.5 and −27.8 kJ/mol, respectively, similarly as found for the van der Waals functionals.

With regard to the general applicability of the hybrid MP2:PBE+D approach used here, we provide information on computer time in the Supporting Information. A single-point calculation for propane/H−CHA can be completed in about 1.5 h on a local four node (16 CPU) compute cluster. Compared to a DFT+D calculation, the CPU time increases by a factor of 10^2. This is substantially less than the increase by a factor of 10^5 reported by Göltl et al.[10] for MP2 calculations on the full periodic structure. This difference of 3 orders of magnitude explains why hybrid QM:QM methods like the ones presented here will continue to be an attractive tool, even if further progress will be made with global algorithmic improvements of wave function methods for periodic structures. There will always be larger systems one wants to tackle, and there will always be more points on the potential energy surface one wants to sample. Our method is perfectly scalable. The size of the high-level cluster can be extended, and the approximation levels can be increased. If MP2 structures are not good enough, one may wish to optimize on a hybrid CCSD(T):MP2 potential energy surface.

6. CONCLUSIONS

For the relevant example of the adsorption of small alkanes at Brønsted sites in H-chabazite, we have shown that free energies for molecule−surface interactions can be calculated ab initio within chemical accuracy limits. To obtain accurate entropies and thermal enthalpy contributions from vibrational partition functions, it is mandatory to take anharmonicity into account, but anharmonic corrections to vibrational frequencies can be calculated for each normal mode separately if finite perturbations of the normal modes are made in an internal coordinate representation.

Whereas for evaluating vibrational contributions, density functional theory with inclusion of dispersion proved to be good enough, for reaching chemical accuracy for the energies of adsorption, a hybrid high-level (MP2) low-level (DFT+D) quantum chemical method was required. The availability of calculated accurate thermal enthalpy contributions and zero-point vibrational energies provides access to experimentally derived (electronic) energies of adsorption, which should serve as benchmarks when testing quantum chemical methods.

The presented methodology permits calculations of both enthalpy and entropy terms for molecule−surface interactions with chemical accuracy that will facilitate atomistic understanding of how different elementary steps act together in heterogeneous catalysis. Future studies will look at the entropy of transition structures and compare different frameworks.

■ ASSOCIATED CONTENT

Supporting Information

Experimental details, XRD patterns, isotherms, and additional IR spectra. Calculated thermodynamic adsorption data for ambient conditions, total energies of optimized structures, computer time, and x,y,z-coordinates of optimized structures. This material is available free of charge via the Internet at http://pubs.acs.org.

■ AUTHOR INFORMATION

Corresponding Authors

*E-mail: js@chemie.hu-berlin.de.
*E-mail: Johannes.lercher@ch.tum.de.

Notes

The authors declare no competing financial interest.

■ ACKNOWLEDGMENTS

This work has been supported by German Science Foundation (DFG) within the priority program 1570 "Porous media" and within the cluster of excellence EXC 314 "Unifying concepts in catalysis", and under the project JE260-10/1. A computer grant from the North German Computing Alliance Berlin− Hannover (HLRN) is also acknowledged. G.P. is a member of the International Max-Planck Research School "Complex surfaces

DOI: 10.1021/acs.jpcc.5b01739
J. Phys. Chem. C 2015, 119, 6128−6137

in materials science" and thanks the Funds of the Chemical Industry for a Kekulé fellowship. We thank Christian Tuma, Berlin, for performing the CCSD(T) calculations.

REFERENCES

(1) Eder, F.; Lercher, J. Alkane Sorption in Molecular Sieves: The Contribution of Ordering, intermolecular Interactions, and Sorption on Bronsted Acid Sites. *Zeolites* **1997**, *18*, 75−81.
(2) Bhan, A.; Gounder, R.; Macht, J.; Iglesia, E. Entropy Considerations in Monomolecular Cracking of Alkanes on Acidic Zeolites. *J. Catal.* **2008**, *253*, 221−224.
(3) Gounder, R.; Iglesia, E. The Roles of Entropy and Enthalpy in Stabilizing Ion-Pairs at Transition States in Zeolite Acid Catalysis. *Acc. Chem. Res.* **2011**, *45*, 229−238.
(4) Campbell, C. T.; Árnadóttir, L.; Sellers, J. R. V. Kinetic Prefactors of Reactions on Solid Surfaces. *Z. Phys. Chem.* **2013**, *227*, 1435.
(5) Campbell, C. T.; Sellers, J. R. V. The Entropies of Adsorbed Molecules. *J. Am. Chem. Soc.* **2012**, *134*, 18109−18115.
(6) Cramer, C. J. *Essentials of Computational Chemistry: Theories and Models*, 2nd ed.; Wiley: Chicester, West Sussex, England, 2004.
(7) Claeyssens, F.; Harvey, J. N.; Manby, F. R.; Mata, R. A.; Mulholland, A. J.; Ranaghan, K. E.; Schuetz, M.; Thiel, S.; Thiel, W.; Werner, H. J. High-accuracy Computation of Reaction Barriers in Enzymes. *Angew. Chem., Int. Ed.* **2006**, *45*, 6856−6859.
(8) Svelle, S.; Tuma, C.; Rozanska, X.; Kerber, T.; Sauer, J. Quantum Chemical Modeling of Zeolite-Catalyzed Methylation Reactions: Toward Chemical Accuracy for Barriers. *J. Am. Chem. Soc.* **2009**, *131*, 816−825.
(9) Hansen, N.; Kerber, T.; Sauer, J.; Bell, A. T.; Keil, F. J. Quantum Chemical Modeling of Benzene Ethylation over H-ZSM-5 Approaching Chemical Accuracy: A Hybrid MP2:DFT Study. *J. Am. Chem. Soc.* **2010**, *132*, 11525−11538.
(10) Göltl, F.; Gruneis, A.; Bucko, T.; Hafner, J. Van der Waals Interactions between Hydrocarbon Molecules and Zeolites: Periodic Calculations at Different Levels of Theory, from Density Functional Theory to the Random Phase Approximation and Moeller-Plesset Perturbation Theory. *J. Chem. Phys.* **2012**, *137*, 114111.
(11) Sillar, K.; Hofmann, A.; Sauer, J. Ab Initio Study of Hydrogen Adsorption in MOF-5. *J. Am. Chem. Soc.* **2009**, *131*, 4143−4150.
(12) Sillar, K.; Sauer, J. Ab Initio Prediction of Adsorption Isotherms for Small Molecules in Metal−Organic Frameworks: The Effect of Lateral Interactions for Methane/CPO-27-Mg. *J. Am. Chem. Soc.* **2012**, *134*, 18354−18365.
(13) Dohnálek, Z.; Kimmel, G. A.; Joyce, S. A.; Ayotte, P.; Smith, R. S.; Kay, B. D. Physisorption of CO on the MgO(100) Surface. *J. Phys. Chem. B* **2001**, *105*, 3747−3751.
(14) Boese, A. D.; Sauer, J. Accurate Adsorption Energies of Small Molecules on Oxide Surfaces: CO-MgO(001). *Phys. Chem. Chem. Phys.* **2013**, *15*, 16481−16493.
(15) Tait, S. L.; Dohnalek, Z.; Campbell, C. T.; Kay, B. D. n-Alkanes on MgO(100). II. Chain Length Dependence of Kinetic Desorption Parameters for Small n-Alkanes. *J. Chem. Phys.* **2005**, *122*, 164708.
(16) Tosoni, S.; Sauer, J. Accurate Quantum Chemical Energies for the Interaction of Hydrocarbons with Oxide Surfaces: CH4/MgO(001). *Phys. Chem. Chem. Phys.* **2010**, *12*, 14330−14340.
(17) Trzesniak, D.; Kunz, A.-P. E.; van Gunsteren, W. F. A Comparison of Methods to Compute the Potential of Mean Force. *ChemPhysChem* **2007**, *8*, 162−169.
(18) Rod, T. H.; Ryde, U. Accurate QM/MM Free Energy Calculations of Enzyme Reactions: Methylation by Catechol O-Methyltransferase. *J. Chem. Theory Comput.* **2005**, *1*, 1240−1251.
(19) Smit, B.; Maesen, T. L. M. Molecular Simulations of Zeolites: Adsorption, Diffusion, and Shape Selectivity. *Chem. Rev.* **2008**, *108*, 4125−4184.
(20) Maesen, T. L. M.; Beerdsen, E.; Calero, S.; Dubbeldam, D.; Smit, B. Understanding Cage Effects in the n-Alkane Conversion on Zeolites. *J. Catal.* **2006**, *237*, 278−290.
(21) Hobza, P.; Sauer, J.; Morgeneyer, C.; Hurych, J.; Zahradník, R. Bonding Ability of Surface Sites on Silica and Their Effect on Hydrogen Bonds. A Quantum Chemical and Statistical Thermodynamic Treatment. *J. Phys. Chem.* **1981**, *85*, 4061−4067.
(22) De Moor, B. A.; Reyniers, M.-F.; Marin, G. B. Physisorption and Chemisorption of Alkanes and Alkenes in H-FAU: A Combined ab Initio-Statistical Thermodynamics Study. *Phys. Chem. Chem. Phys.* **2009**, *11*, 2939−2958.
(23) De Moor, B. A.; Ghysels, A.; Reyniers, M. F.; Van Speybroeck, V.; Waroquier, M.; Marin, G. B. Normal Mode Analysis in Zeolites: Toward an Efficient Calculation of Adsorption Entropies. *J. Chem. Theory Comput.* **2011**, *7*, 1090−1101.
(24) De Moor, B. A.; Reyniers, M. F.; Gobin, O. C.; Lercher, J. A.; Marin, G. B. Adsorption of C2-C8 n-Alkanes in Zeolites. *J. Phys. Chem. C* **2011**, *115*, 1204−1219.
(25) Shang, J.; Li, G.; Singh, R.; Xiao, P.; Danaci, D.; Liu, J. Z.; Webley, P. A. Adsorption of CO2, N2, and CH4 in Cs-Exchanged Chabazite: A Combination of van der Waals Density Functional Theory Calculations and Experiment Study. *J. Chem. Phys.* **2014**, *140*, 084705.
(26) Antony, A.; Hakanoglu, C.; Asthagiri, A.; Weaver, J. F. Dispersion-corrected Density Functional Theory Calculations of the Molecular Binding of n-Alkanes on Pd(111) and PdO(101). *J. Chem. Phys.* **2012**, *136*, 054702.
(27) Van Speybroeck, V.; Van der Mynsbrugge, J.; Vandichel, M.; Hemelsoet, K.; Lesthaeghe, D.; Ghysels, A.; Marin, G. B.; Waroquier, M. First Principle Kinetic Studies of Zeolite-Catalyzed Methylation Reactions. *J. Am. Chem. Soc.* **2011**, *133*, 888−899.
(28) Piccini, G.; Sauer, J. Quantum Chemical Free Energies: Structure Optimization and Vibrational Frequencies in Normal Modes. *J. Chem. Theory Comput.* **2013**, *9*, 5038−5045.
(29) Piccini, G.; Sauer, J. Effect of Anharmonicity on Adsorption Thermodynamics. *J. Chem. Theory Comput.* **2014**, *10*, 2479−2487.
(30) Sauer, J.; Schröder, K.-P.; Termath, V. Comparing the Acidities of Microporous Aluminosilicate and Silico-Aluminophosphate Catalysts: A Combined Quantum Mechanics: Interatomic Potential Function Study. *Collect. Czech. Chem. Commun.* **1998**, *63*, 1394−1408.
(31) Solans-Monfort, X.; Sodupe, M.; Branchadell, V.; Sauer, J.; Orlando, R.; Ugliengo, P. Adsorption of NH_3 and H_2O in Acidic Chabasite, Comparison of ONIOM Approach with Periodic Calculations. *J. Phys. Chem. B* **2005**, *109*, 3539−3545.
(32) Bučko, T.; Benco, L.; Hafner, J.; Ángyán, J. G. Proton Exchange of Small Hydrocarbons over Acidic Chabazite: Ab initio Study of Entropic Effects. *J. Catal.* **2007**, *250*, 171−183.
(33) Vora, B.; Chen, J. Q.; Bozzano, A.; Glover, B.; Barger, P. Various Routes to Methane Utilization—SAPO-34 Catalysis Offers the Best Option. *Catal. Today* **2009**, *141*, 77−83.
(34) Haag, W. O. Catalysis by Zeolites: Science and Technology. In Zeolites and Related Microporous Materials: State of the Art 1994. *Proceedings of the 10th International Zeolite Association Meeting*; Weitkamp, J.; Karge, H. G.; Pfeifer, H.; Hölderich, W., Eds.; Elsevier: Amsterdam, 1994; Vol. *84*, pp 1375−1394.
(35) Tuma, C.; Sauer, J. A hybrid MP2/plane wave-DFT Scheme for Large Chemical Systems: Proton Jumps in Zeolites. *Chem. Phys. Lett.* **2004**, *387*, 388−394.
(36) Tuma, C.; Sauer, J. Treating Dispersion Effects in Extended Systems by Hybrid MP2:DFT Calculations—Protonation of Isobutene in Zeolite Ferrierite. *Phys. Chem. Chem. Phys.* **2006**, *8*, 3955−3965.
(37) Beste, A. One-Dimensional Anharmonic Oscillator: Quantum versus Classical Vibrational Partition Functions. *Chem. Phys. Lett.* **2010**, *493*, 200−205.
(38) Njegic, B.; Gordon, M. S. Exploring the Effect of Anharmonicity of Molecular Vibrations on Thermodynamic Properties. *J. Chem. Phys.* **2006**, *125*, 224102.
(39) Njegic, B.; Gordon, M. S. Predicting Accurate Vibrational Frequencies for Highly Anharmonic Systems. *J. Chem. Phys.* **2008**, *129*, 164107.

DOI: 10.1021/acs.jpcc.5b01739
J. Phys. Chem. C 2015, 119, 6128−6137

(40) De Silva, N.; Njegic, B.; Gordon, M. S. Anharmonicity of Weakly Bound M+−H2 Complexes. *J. Phys. Chem. A* **2011**, *115*, 3272−3278.
(41) Bordiga, S.; Regli, L.; Cocina, D.; Lamberti, C.; Bjørgen, M.; Lillerud, K. P. Assessing the Acidity of High Silica Chabazite H−SSZ-13 by FTIR Using CO as Molecular Probe: Comparison with H−SAPO-34. *J. Phys. Chem. B* **2005**, *109*, 2779−2784.
(42) Eder, F.; Stockenhuber, M.; Lercher, J. A. Bronsted Acid Site and Pore Controlled Siting of Alkane Sorption in Acidic Molecular Sieves. *J. Phys. Chem. B* **1997**, *101*, 5414−5419.
(43) Lercher, J. A.; Noller, H. Infrared Spectroscopic Study of Hydroxyl Group Acid Strength of Silica, Alumina, and Magnesia Mixed Oxides. *J. Catal.* **1982**, *77*, 152−158.
(44) Barrer, R. M.; Davies, J. A. Sorption in Decationated Zeolites. II. Simple Paraffins in H-Forms of Chabazite and Zeolite L. *Proc. R. Soc. London, Ser. A* **1971**, *322*, 1−19.
(45) Eichler, U.; Kölmel, C.; Sauer, J. Combining Ab initio Techniques with Analytical Potential Functions for Structure Predictions of Large Systems: Method and Application to Crystalline Silica Polymorphs. *J. Comput. Chem.* **1997**, *18*, 463−477.
(46) Sierka, M.; Sauer, J. Finding Transition Structures in Extended Systems: A Strategy Based on a Combined Quantum Mechanics: Empirical Valence Bond Approach. *J. Chem. Phys.* **2000**, *112*, 6983−6996.
(47) Boys, S. F.; Bernardi, F. B. The Calculation of Small Molecular Interactions by the Differences of Separate Total Energies. Some Procedures with Reduced Errors. *Mol. Phys.* **1970**, *19*, 553−566.
(48) Halkier, A.; Klopper, W.; Helgaker, T.; Jorgensen, P.; Taylor, P. R. Basis Set Convergence of the Interaction Energy of Hydrogen-Bonded Complexes. *J. Chem. Phys.* **1999**, *111*, 9157−9167.
(49) Jensen, F. Estimating the Hartree—Fock Limit from Finite Basis Set Calculations. *Theor. Chem. Acc.* **2005**, *113*, 267−273.
(50) Helgaker, T.; Klopper, W.; Koch, H.; Noga, J. Basis-set Convergence of Correlated Calculations on Water. *J. Chem. Phys.* **1997**, *106*, 9639−1997.
(51) Alessio, M.; Rybicki, M.; Bischoff, F.; Sauer, J. *Multi-Level Energy Landscapes: The MonaLisa Program*; Humboldt University: Berlin, 2014.
(52) Kresse, G. VASP 5.2.12, http://cms.mpi.univie.ac.at/vasp/vasp/vasp.html, 2012.
(53) Perdew, J. P.; Chevary, J. A.; Vosko, S. H.; Jackson, K. A.; Pederson, M. R.; Singh, D. J.; Fiolhais, C. Atoms, Molecules, Solids, and Surfaces: Applications of the Generalized Gradient Approximation for Exchange and Correlation. *Phys. Rev. B* **1992**, *46*, 6671−6687.
(54) Grimme, S. Semiempirical GGA-type Density Functional Constructed with a Long-Range Dispersion Correction. *J. Comput. Chem.* **2006**, *27*, 1787−1799.
(55) Hättig, C.; Weigend, F. CC2 Excitation Energy Calculations on Large Molecules Using the Resolution of Identity Approximation. *J. Chem. Phys.* **2000**, *113*, 5154−5161.
(56) *TURBOMOLE* V6.5; TURBOMOLE GmbH: Karlsruhe, available from http://www.turbomole.com, 2013.
(57) Dunning, T. H., Jr. Gaussian Basis Sets for Use in Correlated Molecular Calculations. I. The Atoms Boron through Neon and Hydrogen. *J. Chem. Phys.* **1989**, *90*, 1007−1023.
(58) Woon, D. E.; Dunning, T. H., Jr. Gaussian Basis Sets for Use in Correleated Molecular Calculations. III. The Atoms Aluminium through Argon. *J. Chem. Phys.* **1993**, *98*, 1358.
(59) De Silva, N.; Njegic, B.; Gordon, M. S. Anharmonicity of Weakly Bound Li+-$(H_2)_n$ (n = 1−3) Complexes. *J. Phys. Chem. A* **2012**, *116*, 12148−12152.
(60) Kresse, G.; Hafner, J. Ab Initio Molecular Dynamics for Open-Shell Transition Metals. *Phys. Rev. B* **1993**, *48*, 13115.
(61) Kerber, T.; Sierka, M.; Sauer, J. Application of Semiempirical Long-Range Dispersion Corrections to Periodic Systems in Density Functional Theory. *J. Comput. Chem.* **2008**, *29*, 2088−2097.
(62) Dove, M. T.; Harris, M. J.; Hannon, A. C.; Parker, J. M.; Swainson, I. P.; Gambhir, M. Floppy Modes in Crystalline and Amorphous Silicates. *Phys. Rev. Lett.* **1997**, *78*, 1070−1073.
(63) Dove, M. T.; Heine, V.; Hammonds, K. D. Rigid Unit Modes in Framework Silicates. *Mineral. Mag.* **1995**, *59*, 629−639.
(64) Hammonds, K. D.; Deng, H.; Heine, V.; Dove, M. T. How Floppy Modes Give Rise to Adsorption Sites in Zeolites. *Phys. Rev. Lett.* **1997**, *78*, 3701−3704.
(65) Hammonds, K. D.; Heine, V.; Dove, M. T. Rigid-Unit Modes and the Quantitative Determination of the Flexibility Possessed by Zeolite Frameworks. *J. Phys. Chem. B* **1998**, *102*, 1759−1767.
(66) Bates, S. P.; van Well, W. J. M.; van Santen, R. A.; Smit, B. Energetics of n-Alkanes in Zeolites: A Configurational-Bias Monte Carlo Investigation into Pore Size Dependence. *J. Am. Chem. Soc.* **1996**, *118*, 6753−6759.

DOI: 10.1021/acs.jpcc.5b01739
J. Phys. Chem. C 2015, 119, 6128−6137